

A Decision Support System for the Prediction of the Trabecular Fracture Zone

Vasileios Korfiatis, Simone Tassani, and George K. Matsopoulos

Institute of Communication and Computer System,
9 Iroon Polytechniou Street, 157 80, Zografou, Athens, Greece
tassani.simone@gmail.com

Abstract. Prediction of trabecular fracture zone is a very important element for assessing the fracture risk in patients. The assumption that failure always occurs in local bands, the so called ‘fracture zones’, with the remaining regions of the structure largely unaffected has been visually verified. Researchers agreed that the identification of the weakest link in the trabecular framework can lead to the prediction of the fracture zone and consequently of the failure event. In this paper, a decision support system (DSS) is proposed for the automatic identification of fracture zone. Initially, an automatic methodological approach based on image processing is applied for the automatic identification of trabecular bone fracture zone in micro-CT datasets, after mechanical testing. Then, a local analysis of the whole specimen is performed on order to compare the structure (Volumes of Interest -VOI) of the broken region to the unbroken one. As a result, for every VOI, 29 morphometrical parameters were computed and used as initial features to the proposed DSS. The DSS comprises of two main modules: the feature selection module and the classifier. The feature selection module is used for reducing the initial size of the input features’ subset (29 features) and for keeping the most informative features in order to increase the classification’s module performance. To this end, the Sequential Floating Forward Selection (SFFS) algorithm with Fuzzy C-Means evaluation criterion was implemented. For the classification, several classification algorithms including the Multilayer Perceptron (MLP), the Support Vector Machines (SVM), the Naïve Bayesian (NB), the k-Nearest Neighbor (KNN) and the k-Means (KM) have been used. Comparing the performance of these classification algorithms, the SFFS-SVM scheme provided the best performance scoring 98% in terms of overall classification accuracy.

Keywords: Trabecular Fracture Zone, Decision Support Systems, Machine Learning, Feature Selection, Sequential Floating Forward Selection (SFFS), Multilayer Perceptron (MLP), Support Vector Machines (SVM), Naïve Bayesian (NB), k-Nearest Neighbor (KNN), k-Means (KM).

1 Introduction

Prediction of trabecular fracture zone is a wide challenge not yet solved. The cost of fracture treatments related to fracture event are extremely high in Europe and all over the world. The cost related to years of healthy life lost due to disability is also high.

For this reason the right prediction of the fracture zone is a mandatory step for the study and assessment of the fracture risk in patients.

Some in-vitro studies pointed out the importance of local variation of the framework for the global behavior of the whole trabecular structure [1-3]. Researchers agree that the identification of the weakest link in the trabecular framework can lead to the prediction of the fracture zone, first, and of the failure event in general. In a previous study the visual identification of the trabecular fracture zone was used in order to analyze the morphometrical characteristics of the fracture zone and use them to predict the fracture [2]. This approach led to a classification error of about 20%. Nonetheless, the visual identification of the fracture zone limited the study in time and accuracy. Recently an automatic scheme for the identification of the trabecular fracture zone was presented and validated [4]. The automatic tool allowed performing a fast and accurate three-dimensional identification of the broken region. Preliminary results on the morphometry of trabecular fracture were already presented [5]. Authors underline the morphometrical variability of the trabecular structure. The trabecular broken region was found to be a very small part of the whole specimen, and with statistically significant different morphology. Nonetheless, it was not possible to predict the trabecular fracture zone by means of standard statistical tools based on the analysis of parametrical distributions of mean values and standard deviations.

Recent advances in medicine have shown that artificial intelligence (AI) techniques can be used towards the development and application of decision support systems to aid diagnosis [6]. Learning machines have already shown in various fields the capability to recognize different patterns starting from the analysis of specific features [7-11]. Nonetheless, the application of these techniques in the study of trabecular structure was poorly investigated [12], and, to the authors' knowledge, was never applied to the prediction of the trabecular fracture zone using micro-CT images.

The purpose of this paper is to propose a decision support system (DSS) for the prediction of the trabecular fracture zone using the information of structural differences related to the fracture region. The feature selection module is used for reducing the initial size of the input features' subset (29 features) and is comprised by the Sequential Floating Forward Selection (SFFS) algorithm with the Fuzzy C-Means evaluation criterion. Many traditional and well-researched classifiers were implemented and compared during the experimental procedure, including the Multilayer Perceptron (MLP), the Support Vector Machines (SVM), the Naïve Bayesian (NB), the k-Nearest Neighbor (KNN) and the k-Means (KM). These classified each pattern into two distinct classes: the non-fractured and the fractured. Additionally in order to improve the performance of the classification algorithms and reduce the size of the input features, a feature selection (FS) pre-processing stage that used the Sequential Floating Forward Selection (SFFS) algorithm was implemented. The experimental results show that the SVM algorithm using the SFFS feature selector provides almost perfect performance.

2 Materials and Methods

2.1 Data Acquisition

One cylindrical trabecular bone specimen (10mm diameter, 24mm height) was extracted from a human femoral condyle of a donor without skeletal disorders during

the LHDL (IST-2004-026932) European Project [1]. The specimen was scanned at a pixel size of $19.5\mu\text{m}$ by means of a micro-CT (model Skyscan 1072, Skyscan, Kontich, Belgium) and mechanically tested (model Mini bionix 858, MTS Systems Corp., Minneapolis, MN, USA) following a previously published protocol [2, 3,13]. After the mechanical compression the specimen was scanned again in micro-CT obtaining two datasets: pre and post-failure.

2.2 Identification of the Fracture and Non-fracture Zones

An automatic registration scheme for the identification of the full 3D broken region was applied [4, 5]. The used method is a surface-based registration technique which involves the determination and matching of common surfaces of the two sets by the minimization of a distance measure [14]. The method was applied on the pre- and post-failure datasets every specimen. The geometrical transformation employed was the rigid transformation model [15]. The 3D automatic registration method was applied as previously described in literature [4, 5]. Every trabecula was classified as broken or not, based on an overlap criterion described and validated in literature [4]: where a trabecula of the after compression dataset overlap more than 30% with the same trabecula of the before compression dataset all the pixels of that trabecular were classified as unbroken, otherwise they were classified as broken.

2.3 Local Analysis

Preliminary studies already showed the extremely local nature of the trabecular fracture [5, 16]. Therefore, a local analysis of the whole specimen was performed on order to compare the structure of the broken region to the unbroken one. The whole unbroken dataset constitutes of a stack of $469 \times 469 \times 991$ voxels and it was divided in 1134 cubic volume of interests (VOIs). Every VOI was $93 \times 93 \times 93$ voxels and they had an overlap of 46 voxel in all the three dimensions (2D application is shown in Fig. 1).

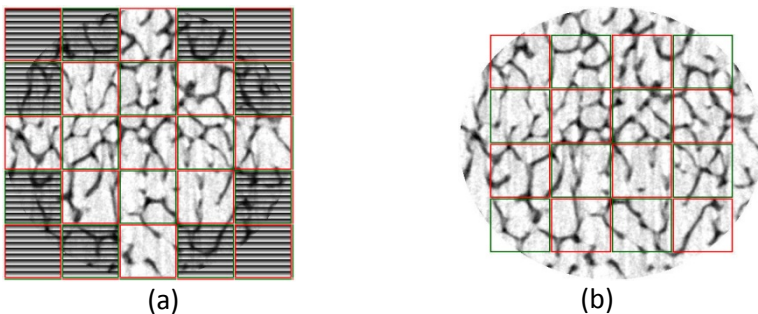


Fig. 1. Two dimensional projection of the VOIs selection is shown. a) The specimen was split in cubes. VOIs heaving less than 80% of the volume covered by the cylindrical shape of the specimen were not included in the analysis (shadowed VOIs). b) Translation of the VOIs in x and y is shown.

Due to the cylindrical shape of the specimen, not all the obtained VOIs were suitable for the morphometric analysis. Only VOIs having at least 80% of the volume covered by the cylindrical shape of the specimen were selected (Fig. 1a). The morphometric analysis was finally performed only on the actual tissue volume, defined by the cylindrical geometry of the specimen (i.e. the white part in four corner volumes in Fig. 1b was not included in the tissue study).

2.4 Feature Description

For every VOI, 29 morphometrical parameters were computed. These include 1.tissue volume (TV), 2.bone volume (BV), 3.bone surface (BS), 4.bone volume fraction (BV/TV), 5.bone surface to volume ratio (BS/BV), 6.bone surface density (BS/TV), 7.direct trabecular thickness (Tb.Th*), 8.direct trabecular separation (Tb.Sp*), 9.structure model index (SMI), 10.connectivity density (CD), 11-13.the eigenvalues (E1, E2, and E3) and 14-22.eigenvectors' coordinates of the fabric tensor, 23-25.their normalizations (H1, H2, and H3), 26.the off-axis angle, 27-28.two degrees of anisotropy (DA₁ and DA₂) and 29.the ellipsoid correlation coefficient (CC). The normalized eigenvalues were computed using the normalization proposed by Turner et al. [17], obtained from the three principal directions of the ellipsoid. The above parameters were used as input features for the proposed DSS and were calculated for the VOIs of each specimen using the software "CtAnalyzer" (Skyscan, Kontich, Belgium).

Tissue Volume (TV) is the total volume of every volume-of-interest (VOI). The 3D volume measurement is based on the marching cubes volume model of the VOI. Bone Volume (BV) is the total volume of binarized objects of the foreground within the VOI or in other words the sum of voxels marked as bone. Bone Surface (BS) is the surface area of all the solid objects within the VOI, measured in 3D (Marching cubes method). The calculation of the BV/TV, BS/BV and BS/TV was also used as features.

The Tb.Th*, based on the estimation of volume-based local thickness independently of an assumed structure type, was calculated using the sphere-fitting method [18]. Tb.Sp* is defined as the diameter of the marrow cavities, and was calculated using the same technique described for Tb.Th*[12]. The SMI is a topological index, giving an estimation of the characteristic form in terms of plates and rods composing the 3D structure. For ideal plates and rods, the index gives respectively the values 0 and 3, whereas for a mixed structure the SMI-index lies in between 0 and 3 [19]. The connectivity density is a parameter to measure the degree of multiple connections, and hence reports the maximal number of branches that can be broken in a network before the structure is separated into two parts [20]. The term fabric was introduced in bone mechanics as a description of the anisotropy of a material's microstructure [21]. The fabric tensor was defined as a positive second rank tensor which quantitatively describes fabric [21, 22].

The eigenvalues of the fabric tensor (E_i) were obtained using the mean intercept length (MIL) technique [23, 24]. Using this technique a grid of parallel line is superimposed to the trabecular structure. The average distance between interceptions of the grid with the trabecular structure is computed and plotted in 3D. If the structure is orthotropic (three axis of symmetry) the distribution can be approximated to an

ellipsoid. The values of E_1 , E_2 , and E_3 represent the principal axes in three dimensions (3D) of the ellipsoid. These values give information about how distant the trabeculae are in the three dimensions, and therefore how oriented the framework is in every direction. These eigenvalues and the consequent eigenvectors' coordinates (which are the 3x3 fabric tensor matrix's values) give twelve features in total. E_i were shown to be dependent from other structural parameters (e.g. the porosity of the structure) [25], therefore the normalization of the eigenvalues was also used. Normalized eigenvalues (H_i) were obtained from the three principal directions of the ellipsoid, using the normalization proposed by Turner et al. [17]:

$$H_1 \pm H_2 \pm H_3 = 1 \quad (1)$$

Degree of anisotropy (DA) is a measurement of the anisotropy of the 3D object. Anisotropy is a measure of 3D asymmetry along a particular directional axis. Apart from percent volume, DA and the general stereology parameters of trabecular bone are probably the most important determinants of mechanical strength [22]. The two DAs analyzed are the ones suggested in the literature [26, 27] and were computed as a ration between the three principal MILs:

$$DA_1 = MIL_1/MIL_3 \quad (2)$$

$$DA_2 = MIL_2/MIL_3 \quad (3)$$

The off axis angle was defined as the difference between the main trabecular direction of the analyzed VOI, identified by the direction of the principal eigenvector, and the load direction. Finally, the CC's value corresponds to the fitting of the ideal ellipsoid to the experimental one.

2.5 Proposed Decision Support System

The proposed decision support system (DSS) is comprised by the following modules (Fig. 2):

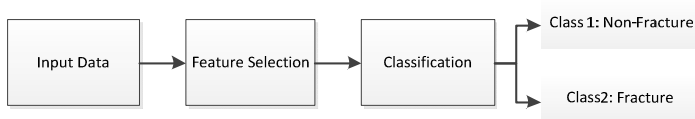


Fig. 2. The proposed DSS

The input data consists of 734 patterns in total. From these 453 belong to the non-fractured class and 281 to the fractured class, providing an approximate ratio of 60/40% non-fractured/fractured patterns. The original data set contained 1134 patterns, which represent the VOIs of the specimen, but its composition was very unbalanced in favor of the non-fractured class. As a result 400 patterns from the non-fractured class were randomly removed, and the rest 734 were fed to the proposed DSS.

The feature selection module is used for reducing the initial size of the input features' subset (29 features) and for keeping the most informative features in order to increase the classification's module performance. To this end, the Sequential Floating Forward Selection (SFFS) algorithm [28] with Fuzzy C-Means [29] evaluation criterion was implemented. This algorithm starts with a feature subset of a certain predetermined size and moves up or down in number in order to find the best composition. It usually converges to a local minimum, thus is considered suboptimal. The feature subset that the algorithm returns generally tries not to deviate much in size from the given starting size. For the experimental procedure the number of epochs was set to 100 and the number of starting features was set to four values, 5, 10, 15 and 20.

In the classification module, five well-established classification algorithms were implemented including the Multilayer Perceptrons (MLP) [30], Support Vector Machines (SVM)[31], Naïve Bayesian (NB)[32], k-nearest neighbor (KNN)[32] and k-means clustering (KM)[33]. The MLP had one hidden layer with 20 neurons and used the linear transfer function for the first stage (input-hidden) and the hyperbolic tangent sigmoid transfer function for the second stage (hidden-output). For its training the error back-propagation technique with the Levenberg-Marquardt optimization was used. The SVM used the Sequential Minimal Optimization (SMO) technique for finding the separating hyperplane and the linear kernel function (dot product) for mapping the training data into kernel space. For the NB the kernel smoothing density estimate was used for modelling the distribution of the data. The kernel used was the normal (Gaussian) kernel and the width was selected automatically from the Matlab 2011b software for each class and feature. The prior probabilities for the classes were specified using the empirical rule which takes into account the relative frequencies of the classes in training. The KNN classifier used the nearest neighbor only ($k=1$) and the Euclidean distance for classifying the test data. Finally, for the KM the number of centroids was set to $k=2$ since the problems consists of two classes and the distance measure used was the Squared Euclidean with an online update phase.

For the supervised learning algorithms (MLP, SVM, NB and KNN) the cross-validation training procedure [34] was used in order to provide convenient statistical quality of the results. The data set was randomly broken down into five groups so that each group contained 1/5 of the total given patterns. As a result, the technique was five-fold cross-validation and the training-test ratio was 80/20%. For each of the five repetitions, one of the groups was considered the test set and the other four merged and created the training set. The mean values from all five repetitions formed the final values of the measures for each algorithmic scheme.

For the unsupervised learning KM, there are no training and test sets and all the selected features are fed to the algorithm. The algorithm starts with the two centroids in random locations and then assigns each pattern to the closest centroid according to the selected distance measure, creating the two clusters. It then changes the positions of the two centroids in the feature space to the average location of the selected patterns of each and repeats the above procedure. It finishes when no change in the centroids' coordinates is made. For the evaluation of the results the true labels of the patterns were compared to the labels (clusters) that the KM assigned. Since the class-cluster assignment is interchangeable for each algorithmic run, the assignment that provided the higher value of the evaluation measure was considered valid each time.

2.6 Evaluation Measures

Based on the confusion matrices of each classifier scheme the accuracy, the sensitivity and the specificity were calculated using the following equations:

$$Accuracy = \frac{Number\ of\ Instances\ Labeled\ Correctly}{Total\ number\ of\ Instances} \tag{4}$$

$$Sensitivity = \frac{True\ Positives}{True\ Positives + False\ Negatives} \tag{5}$$

$$Specificity = \frac{True\ Negatives}{True\ Positives + False\ Positives} \tag{6}$$

In simpler terms sensitivity measures how precise is the classifier in predicting the class A, which is the non-fractured in our experiment and the specificity the same for class B, which is the fractured. We also used ROC space representation in order to more accurately assess the quality of the implemented classifiers.

For the experiments an Intel Q9450@2.66 GHz CPU, 4GB DDR2 RAM PC running on Windows 7 OS was used. All machine learning techniques were developed using Matlab 2011b.

3 Results

The best system performance is obtained using the SFFS with 15 features and the SVM algorithm. In that case, the sensitivity 99%, the specificity 95% and the total accuracy is 98%. Fig. 3 is a multiple column graph that contains the visualisations of the percent measurements of accuracy, sensitivity and specificity for the five implemented classifiers. These are the mean values from 5 repetitions. Each measure is represented by a different shade of grey. That information is illustrated simultaneously for all the different feature selection scenarios that were tried out (5, 10, 15 and 20 starting features) and for the scenario that no feature selection was used.

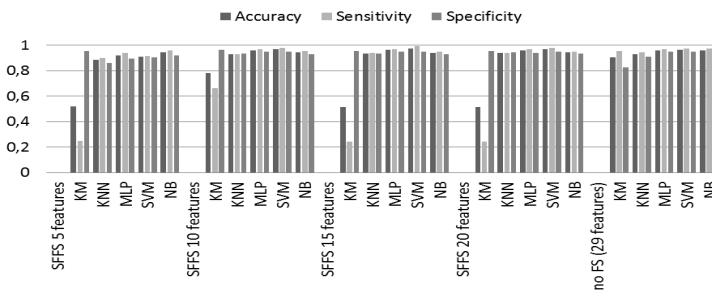


Fig. 3. Experimental results for the various classification scenarios

In Table 1, the confusion matrices of the classification for the best feature scenario (15 features) are provided. These results are the mean values of 5 different algorithm executions. Rows correspond to the real labels and columns to the classifier’s labels. Class 1 is the name of the non-fractured class (90 test-patterns for each iteration) and class 2 of the fractured one (56 test-patterns for each iteration). The KM clustering is a non-supervised classification algorithm and as a result the total number of patterns is taken into account. From the Table 1, it is evident that the SVM shows the best performance.

Table 1. Confusion Matrix for SFFS-15 Features Averaged Over 5 Independent Algorithm Executions

Method	Actual class	Predicted class	
		Class 1	Class 2
KM	Class 1	111	342
	Class 2	13	268
KNN	Class 1	86	3.8
	Class 2	4.6	52.4
MLP	Class 1	87.8	2.8
	Class 2	2.8	53.4
SVM	Class 1	90.2	3
	Class 2	0.4	53.2
NB	Class 1	86.2	3.8
	Class 2	4.4	52.4

In Fig.4, the ROC curves of the classifiers for the SFFS with 15 features are shown. In the Y-axis is the True Positive Rate (TPR) which is equal to the Sensitivity and in the X-axis is the False Positive Rate (FPR) which is equal to (1-Specificity). These curves prove again that the SVM is the best classifier followed closely by the MLP and the rest of the supervised classifiers.

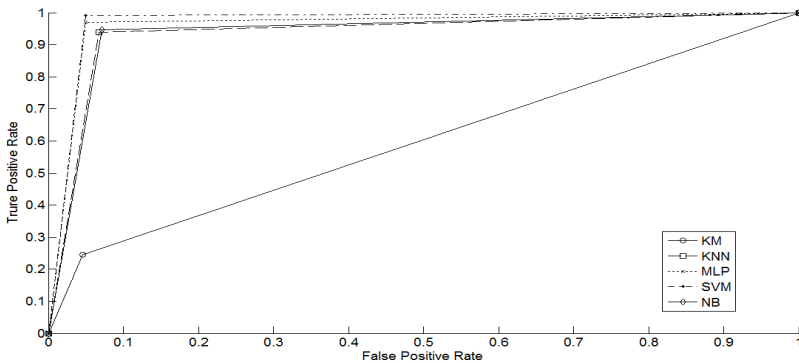


Fig. 4. ROC curves

4 Discussion

Trabecular fracture is a much localized event. This scenario brought a natural imbalance between the numbers of gathered samples that belonged to the non-fractured class and those that belonged to the fractured class, with the first being much greater than the second. The original dataset contained 1134 patterns from which 853 belonged to the non-fractured class and 281 to fractured class, striking a ration of approximately 75-25%. It is common knowledge though that the two most important attributes of a good data set are having a big number of patterns and striking a balanced ratio among the different classes. As a result, 400 patterns that belonged to the non-fractured class were removed, but all the patterns that belonged to the fractured class were kept, producing the final experimental data set that was described earlier. This choice greatly enhanced the quality of the classifiers in every aspect.

The feature selection stage was implemented in an attempt to improve the system's performance and at the same time investigate the impact of the several input features on the classification procedure. The important parameters of the SFFS are the number of starting features (input features' subset size) and the number of epochs, which represents the maximum allowed repetitions in case the algorithm does not converge in a minimum. The experimental results show clearly that the general performance of all the supervised classifiers is slightly affected by the presence of a feature selection system. For example, the SVM's accuracy was 91% for 5 starting features, 96% for 10 starting features, 98% for 15 starting features (best case) and 96% for 20 starting features. The other supervised classifiers showed even smaller deviation as the features' number increased but still could not outperform the SVM. The performance of the KM clustering (unsupervised) showed great variance in terms of the starting feature parameter's value. Its results remain poor though except from the case when no FS is used; then they are acceptable but still inferior from the rest. Considering the features number it seems that the best option is around 15 features. Much lower values of the starting features parameter decrease the performance whereas higher values do not provide any significant improvement. The algorithms always converged within the given number of epochs. Its running time was analogous of the starting features and was about 2 minutes for the 15 starting features case.

In fig.5 the frequency of selection for each input feature is illustrated. Consulting the numbering given in the feature presentation in Chapter 2 the most important features, appear to be the direct Tb.Th, the direct Tb.Sp, the BV and the 'y' component of the 'y' eigenvector , which were selected every time the SFFS algorithm run.

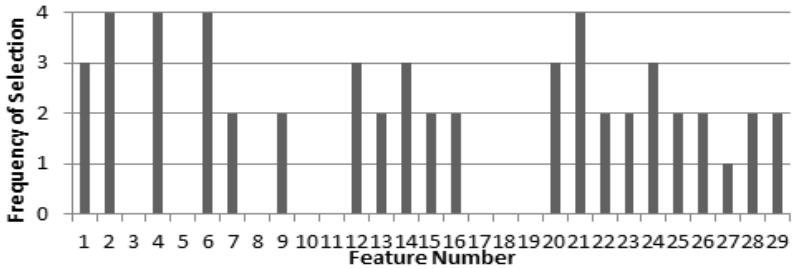


Fig. 5. Frequency of selection for each feature

Finally, it has to be noted that the only FS algorithm that was implemented was the SFFS. As a result it is possible that other FS algorithms may provide better performance and/or indicate other features as important. Nonetheless, it is important to notice that, among the 4 parameters always selected by the SFFS, 3 are related to the amount of tissue and only one is related to the orientations of the structure. However, the meaning of Tb.Th and Tb.Sp analyzed together is related to the number of trabeculae within the analyzed VOI. Therefore, it is suggested that the number of trabeculae, the amount of bone and the orientation of the structure are the most important parameters, leaving out of the discussion the anisotropy of the tissue, the connectivity of the structure and the plate/rod shape of the trabeculae. Nonetheless, even if 734 specimens were analyzed, we must remember that the whole study is related to the analysis of only one physical specimen. A bigger sample size should be analyzed before any reliable physical meaning could be carried out.

The importance of the features seems the most interesting topic though since the performance achieved without the FS stage is generally very good (over 90% accuracy for all implemented schemes). Nonetheless, FS is a mandatory step in order to move to the clinical domain. Micro-CT images of in-vitro specimens allow to perform very accurate analysis and to compute a great number of parameters. However, it is strongly improbable to be able, even in the future, to perform such in deep analysis on clinical images. For this reason it is important to identify the most important parameters and find a way to compute the same parameters in clinics.

Considering the optimal classifier the 15 features scheme will be taken into account. In that case the performance of all the supervised classifiers is very good but the most robust and efficient option for this binary classification problem seems to be the SVM. It performed almost perfectly and needed in general very low amount of training time (about 1 second). Concerning the MLP training time the number of epochs it needed was around 10, a very low number as well. It has to be noted that the unsupervised KM clustering performed worse than all the supervised schemes, mainly because it showed a clear tendency in classifying the majority of the patterns to the fractured class.

References

1. Tassani, S., Ohman, C., Baruffaldi, F., Baleani, M., Viceconti, M.: Volume to density relation in adult human bone tissue. *J. Biomech.* 44, 103–108 (2011)
2. Perilli, E., Baleani, M., Ohman, C., Fognani, R., Baruffaldi, F., Viceconti, M.: Dependence of mechanical compressive strength on local variations in microarchitecture in cancellous bone of proximal human femur. *J. Biomech.* 41, 438–446 (2008)
3. Tassani, S., Ohman, C., Baleani, M., Baruffaldi, F., Viceconti, M.: Anisotropy and inhomogeneity of the trabecular structure can describe the mechanical strength of osteoarthritic cancellous bone. *J. Biomech.* 43, 1160–1166 (2010)
4. Tassani, S., Asvestas, P.A., Matsopoulos, G.K., Baruffaldi, F.: Automatic Identification of Trabecular Bone Fracture. In: Bamidis, P.D., Pallikarakis, N. (eds.) *MEDICON 2010. IFMBE Proceedings*, vol. 29, pp. 296–299. Springer, Heidelberg (2010)
5. Tassani, S., Demenegas, F., Matsopoulos, G.K.: Local analysis of trabecular bone fracture. In: *Conf. Proc. IEEE Eng. Med. Biol. Soc.*, pp. 7454–7457 (2011)
6. Leroy, G., Chen, H.: Introduction to the special issue on decision support in medicine. *Decision Support Systems* 43, 1203–1206 (2007)
7. Palaniswami, M.: Computational Intelligence in Gait Research: A Perspective on Current Applications and Future Challenges. *IEEE Transactions on Information Technology in Biomedicine* 13(5), 687–702 (2009)
8. Mashor, M.Y., Jaafar, H.: Online sequential extreme learning machine for classification of mycobacterium tuberculosis in ziehl-neelsen stained tissue. In: *2012 International Conference on Biomedical Engineering*, February 27–28, pp. 139–143 (2012)
9. Pena, E., Martínez, M.A.: Machine Learning Techniques as a Helpful Tool Toward Determination of Plaque Vulnerability. *IEEE Transactions on Information Technology in Biomedicine* 59(4), 1155–1161 (2012)
10. Madokoro, H., Otani, T., Kadowaki, S.: Experimental studies with a hybrid model of unsupervised neural networks. In: *The 2011 International Conference on Neural Networks (IJCNN)*, July 31–August 5, pp. 1659–1666 (2011)
11. Phlypo, R., Congedo, M.: SVM feature selection for multidimensional EEG data. In: *IEEE International Conference on Acoustics, Speech and Signal Processing (ICASSP)*, May 22–27, pp. 781–784 (2011)
12. Christopher, J.J., Ramakrishnan, S.: Assessment and classification of mechanical strength components of human femur trabecular bone using texture analysis and neural network. *J. Med. Syst.* 32, 117–122 (2008)
13. Ohman, C., Baleani, M., Perilli, E., Dall’Ara, E., Tassani, S., Baruffaldi, F., Viceconti, M.: Mechanical testing of cancellous bone from the femoral head: experimental errors due to off-axis measurements. *J. Biomech.* 40, 2426–2433 (2007)
14. Matsopoulos, G.K., Delibasis, K.K., Mouravliansky, N.A., Asvestas, P.A., Nikita, K.S., Kouloulias, V.E., Uzunoglu, N.K.: CT-MRI automatic surface-based registration schemes combining global and local optimization techniques. *Technol. Health Care* 11, 219–232 (2003)
15. van den Elsen, P.A., Pol, E.J.D., Viergever, M.A.: Medical image matching—a review with classification. *IEEE Engineering in Medicine and Biology Magazine* 12, 26–39 (1993)
16. Tassani, S., Demenegas, F., Matsopoulos, G.K.: Morphometry of trabecular bone fracture: preliminary study. In: *XXIIIrd Congress of the International Society of Biomechanics*, July 3–7, p. 69. International Society of Biomechanics, Brussels (2011)
17. Turner, C.H., Cowin, S.C., Rho, J.Y., Ashman, R.B., Rice, J.C.: The fabric dependence of the orthotropic elastic constants of cancellous bone. *J. Biomech.* 23, 549–561 (1990)

18. Hildebrand, T., Ruegsegger, P.: A new method for the model-independent assessment of thickness in three-dimensional images. *Journal of Microscopy* 185, 67 (1997)
19. Hildebrand, T., Ruegsegger, P.: Quantification of Bone Microarchitecture with the Structure Model Index. *Comput. Methods Biomech. Biomed. Engin.* 1, 15–23 (1997)
20. Odgaard, A., Gundersen, H.J.: Quantification of connectivity in cancellous bone, with special emphasis on 3-D reconstructions. *Bone* 14, 173–182 (1993)
21. Cowin, S.C.: The relationship between the elasticity tensor and the fabric tensor. *Mechanics of Materials* 4, 137 (1985)
22. Odgaard, A.: Three-dimensional methods for quantification of cancellous bone architecture. *Bone* 20, 315–328 (1997)
23. Harrigan, T.P., Mann, R.W.: Characterization of microstructural anisotropy in orthotropic materials using a second rank tensor. *Journal of Materials Science* 19, 761 (1984)
24. Whitehouse, W.J.: The quantitative morphology of anisotropic trabecular bone. *J. Microsc.* 101, 153–168 (1974)
25. Tassani, S., Particelli, F., Perilli, E., Traina, F., Baruffaldi, F., Viceconti, M.: Dependence of trabecular structure on bone quantity: a comparison between osteoarthritic and non-pathological bone. *Clin. Biomech. (Bristol, Avon)* 26, 632–639 (2011)
26. Goulet, R.W., Goldstein, S.A., Ciarelli, M.J., Kuhn, J.L., Brown, M.B., Feldkamp, L.A.: The relationship between the structural and orthogonal compressive properties of trabecular bone. *J. Biomech.* 27, 375–389 (1994)
27. Majumdar, S., Kothari, M., Augat, P., Newitt, D.C., Link, T.M., Lin, J.C., Lang, T., Lu, Y., Genant, H.K.: High-resolution magnetic resonance imaging: three-dimensional trabecular bone architecture and biomechanical properties. *Bone* 22, 445–454 (1998)
28. Pudil, P., Novovicova, J., Kittler, J.: Floating search methods in feature selection. *Pattern Recognition Letters* 15, 1119–1125 (1994)
29. Nock, R., Nielsen, F.: On Weighting Clustering. *IEEE Trans. on Pattern Analysis and Machine Intelligence* 28(8), 1–13 (2006)
30. Rosenblatt, F.: *Principles of Neurodynamics: Perceptrons and the Theory of Brain Mechanisms*. Spartan Books, Washington, DC (1961)
31. Cortes, C., Vapnik, V.N.: Support-Vector Networks. *Machine Learning* 20 (1995)
32. Theodoridis, S., Koutroumbas, K.: *Pattern Recognition*, 4th edn. Elsevier Inc. (2009)
33. Lloyd, S.P.: Least squares quantization in PCM. *IEEE Transactions on Information Theory* 28(2), 129–137 (1982)
34. Devijver, P.A., Kittler, J.: *Pattern Recognition: A Statistical Approach*. Prentice-Hall, London (1982)